

---

---

## **REPORT No. 259**

---

### **CHARACTERISTICS OF PROPELLER SECTIONS TESTED IN THE VARIABLE DENSITY WIND TUNNEL**

By EASTMAN N. JACOBS

Langley Memorial Aeronautical Laboratory



# REPORT No. 259

## CHARACTERISTICS OF PROPELLER SECTIONS TESTED IN THE VARIABLE DENSITY WIND TUNNEL

By EASTMAN N. JACOBS

### SUMMARY

Tests were carried out in the variable density wind tunnel of the National Advisory Committee for Aeronautics on six airfoil sections used by the Bureau of Aeronautics as propeller sections. The sections were tested at pressures of 1 and 20 atmospheres corresponding to Reynolds Numbers of about 170,000 and 3,500,000. The results obtained, besides providing data for the design of propellers, should be of special interest because of the opportunity afforded for the study of scale effect on a family of airfoil sections having different thickness ratios.

### DESCRIPTION OF TESTS

A description of the tunnel and of the general methods of testing airfoils may be found in Reference 1. The usual 5 by 30-inch duralumin airfoils were used. The models have flat lower surfaces and the maximum thickness at one-third of the chord from the leading edge. The radius of the leading edge is one-tenth of the maximum ordinate. The maximum ordinates are: 0.04, 0.08, 0.10, 0.12, 0.16, and 0.20 of the chord. The ordinates of all of the sections may be obtained from those of the thickest section by reducing all of the ordinates in the same ratio as the maximum ordinate. The ordinates of all of the upper surfaces are given in Table I.

Tests were carried out on each airfoil to determine the lift, drag, and moment coefficients at different angles of attack. The tests were made at pressures of approximately 1 and 20 atmospheres, giving Reynolds Numbers of about 170,000 and 3,500,000.

### RESULTS AND DISCUSSION

Figures 1 and 2 are the curves of lift coefficients plotted against angle of attack for all sections. Those in Figure 1 are from the 1 atmosphere tests and those in Figure 2, from the 20 atmosphere tests. These curves show the effect of changing the thickness of a section at a low Reynolds Number and at a high Reynolds Number.

Figures 3 and 4 are the curves of lift coefficients plotted against drag coefficients for all sections, from the 1 and 20 atmosphere tests, respectively. These curves show that the profile drag increases uniformly with thickness, over the range where it is fairly constant, for both the small and the large Reynolds Number tests. However, the range of constant profile drag is greater at the large Reynolds Number. The extremely low drag measured for the thinnest airfoil may be erroneous since it was set up differently.

In the same manner, curves of drag per unit lift ( $D/L$ ) are drawn in Figures 5 and 6. The straight line representing the induced drag per unit lift for aspect ratio 6 is plotted on the same sheets.

The next set of curves, Figures 7 to 12, show the complete characteristics and also the scale effect on each section by means of the drag (polar curves), and moment coefficient plotted against lift coefficient. The solid curves represent the 20-atmosphere tests and the dotted curves the 1-atmosphere tests. The same data will be found in tabular form in the Tables numbered III to XIV.

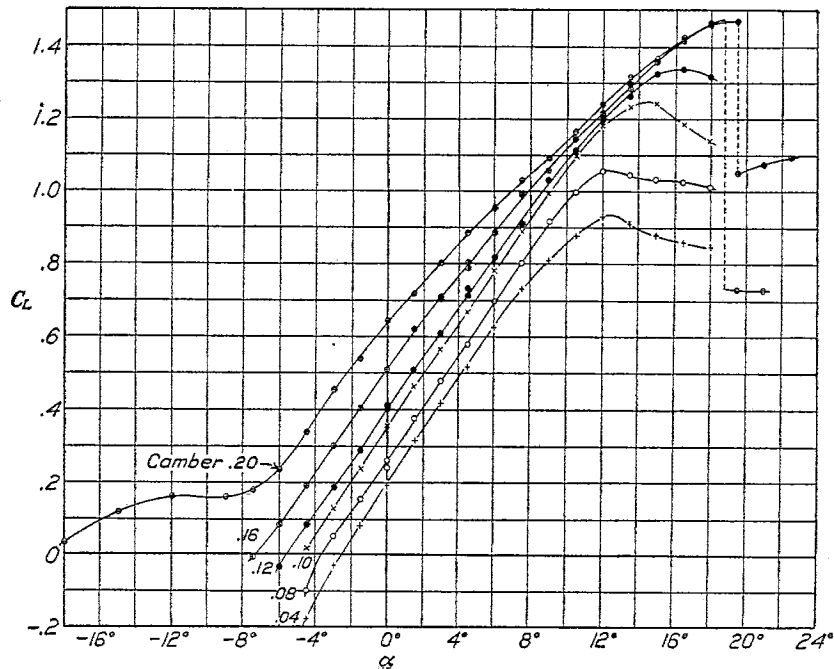


FIG. 1.—Lift curves from tests at 1 atmosphere

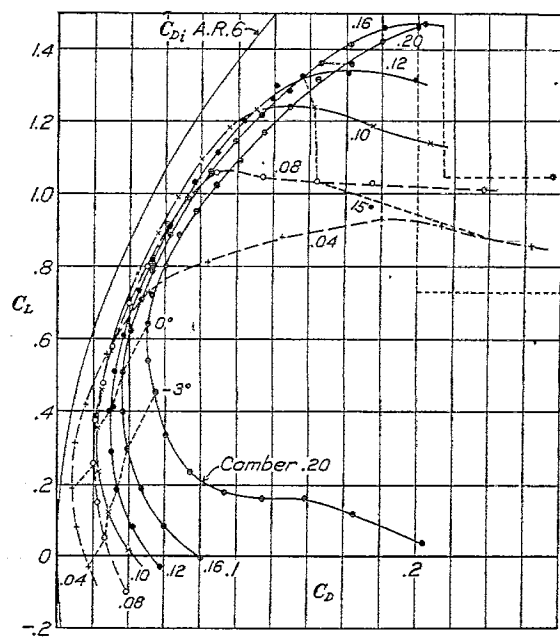


FIG. 2.—Polar curves from tests at 1 atmosphere

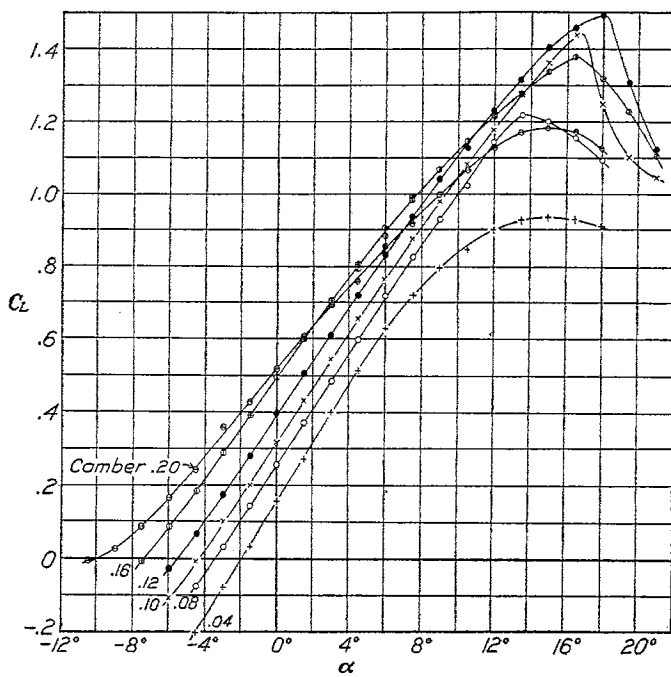


FIG. 3.—Lift curves from tests at 20 atmospheres

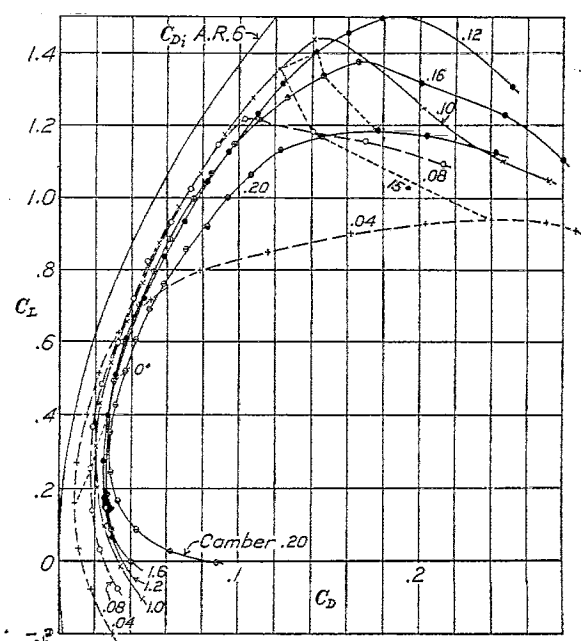


FIG. 4.—Polar curves from tests at 20 atmospheres

The remaining curves, Figures 13 to 18, represent the variation of lift coefficient, drag coefficient, and  $\frac{L}{D}$  with angle of attack. The results from both the high and low Reynolds Number tests are plotted on the same sheet in order to show the scale effect on each section. We may conclude from these curves that there is little scale effect on either slope of the lift curve or angle of zero lift except for the thickest section where the slope of the lift curve is considerably below normal and the angle of zero lift is effected by burbling, which probably exists at all angles of attack. The two thickest sections at one atmosphere show a discontinuity of flow at maximum lift and give a lower maximum lift without the discontinuity at 20 atmospheres. The moderately thick airfoils all give a higher maximum lift at the higher Reynolds Number.

As regards scale effect on the drag, it may be concluded that, below maximum lift, the drag at any angle of attack is either reduced or not changed at all as the Reynolds Number is increased from 170,000 to 3,500,000. There is an exception for the two thickest sections at angles just below the discontinuity of flow at maximum lift where the drag is lower at the lower Reynolds Number. In general, the scale effect is small for efficient sections over the range of angles where the sections have a low profile drag.

Previous tests have been made to determine the characteristics and scale effect for these propeller sections. In the tests covered by References 3 and 4 the dynamic scale was increased by increasing the velocity to very high values. However, the range of Reynolds Numbers was not as great and the conditions of the tests were so different that a comparison of the results here is not justified.

The tendency of the drag to increase at low and negative angles of attack indicates a breaking away of the flow from the lower surface of the airfoil. Although the effect is less at the higher Reynolds Number, it could probably be eliminated altogether by the substitution of a leading edge similar to that of the Clark Y.

Before the models were tested some of their characteristics were calculated from their sections. The

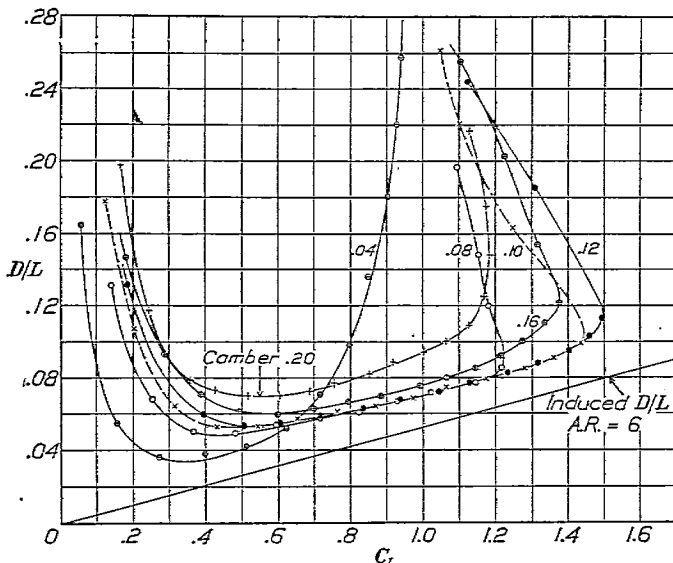


FIG. 5.— $D/L$  curves from tests at 1 atmosphere

moment coefficient about the quarter chord point from the leading edge and the angle of zero lift were calculated by a method based on Munk's integrals and outlined in

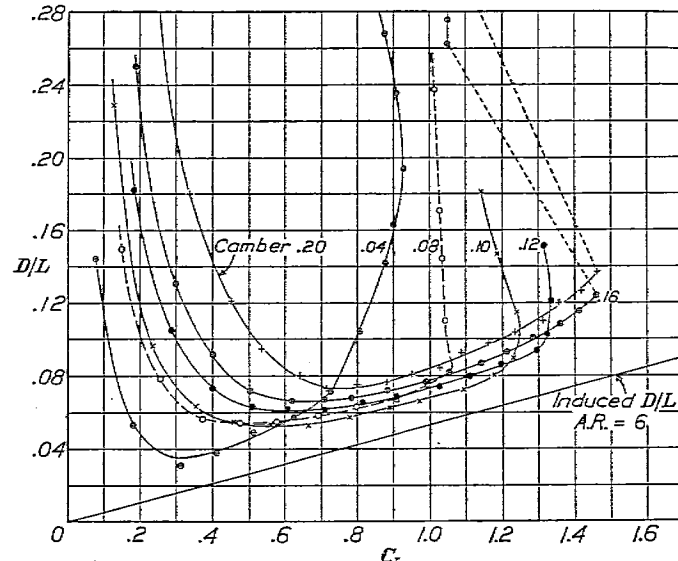
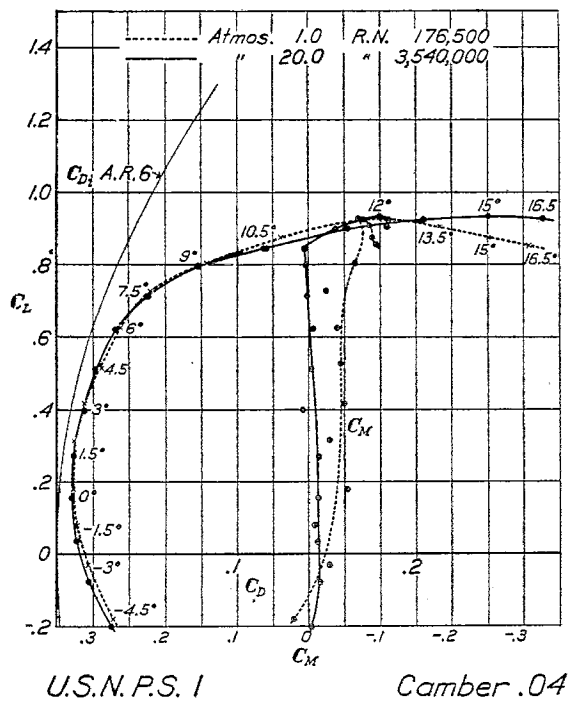
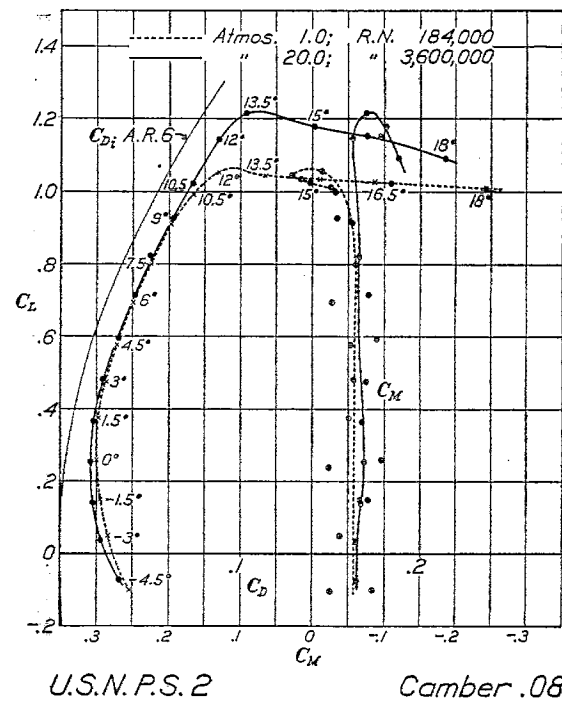


FIG. 6.— $D/L$  curves from tests at 20 atmospheres



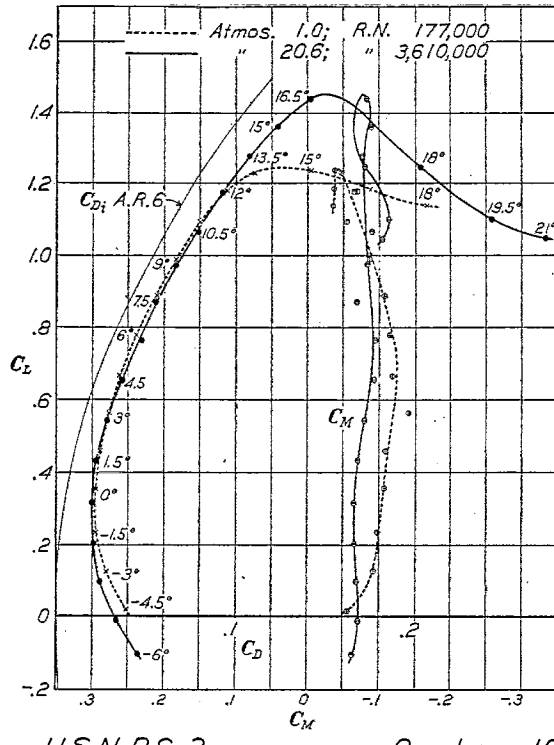
U.S.N.P.S. 1 Camber .04



U.S.N.P.S. 2 Camber .08

FIG. 7.—Polar and moment curves of U. S. N. P. S. 1 at different values of R. N.

FIG. 8.—Polar and moment curves of U. S. N. P. S. 2 at different values of R. N.



U.S.N.P.S. 3 Camber .10

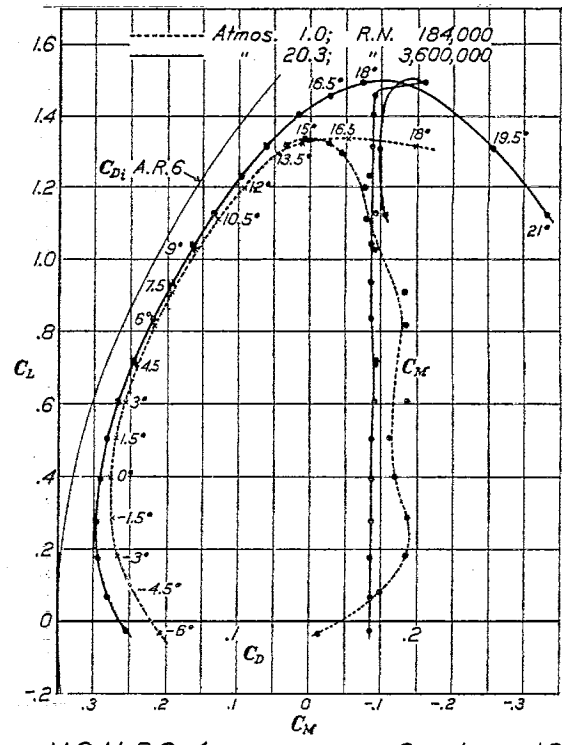


FIG. 9.—Polar and moment curves of U. S. N. P. S. 3 at different values of R. N.

FIG. 10.—Polar and moment curves of U. S. N. P. S. 4 at different values of R. N.

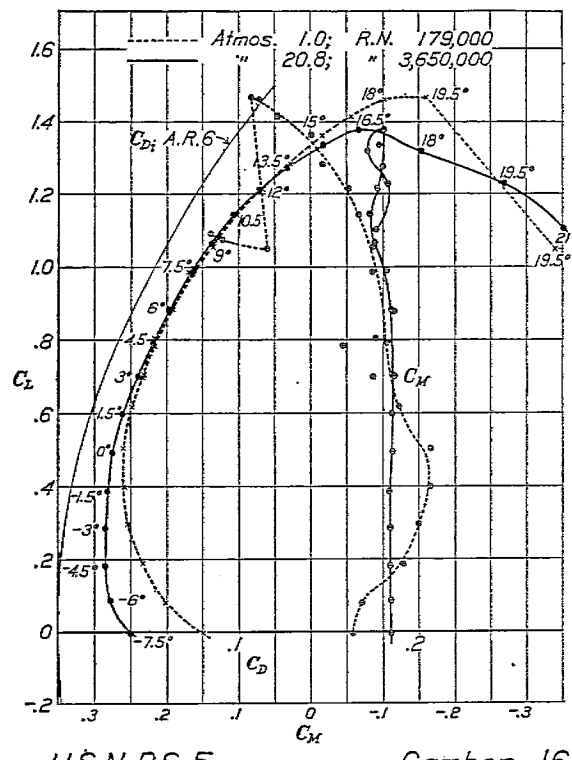


FIG. 11.—Polar and moment curves of U. S. N. P. S. 5 at different values of R. N.

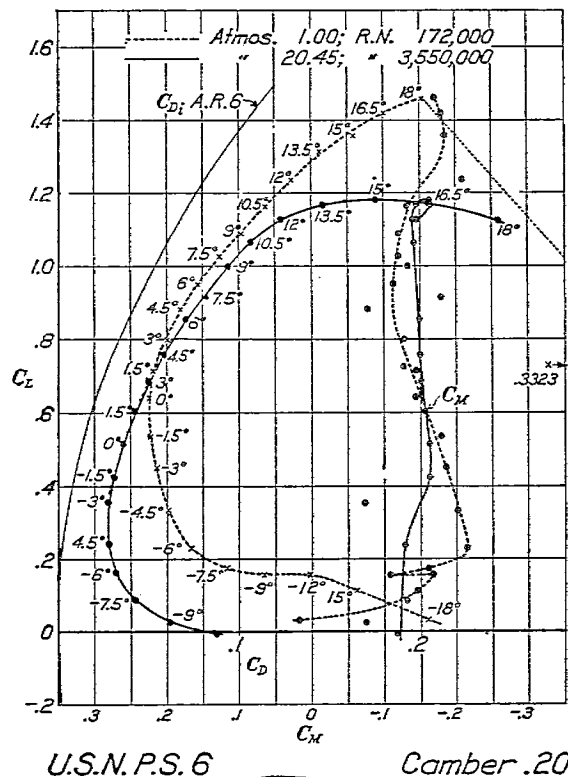


FIG. 12.—Polar and moment curves of U. S. N. P. S. 6 at different values of R. N.

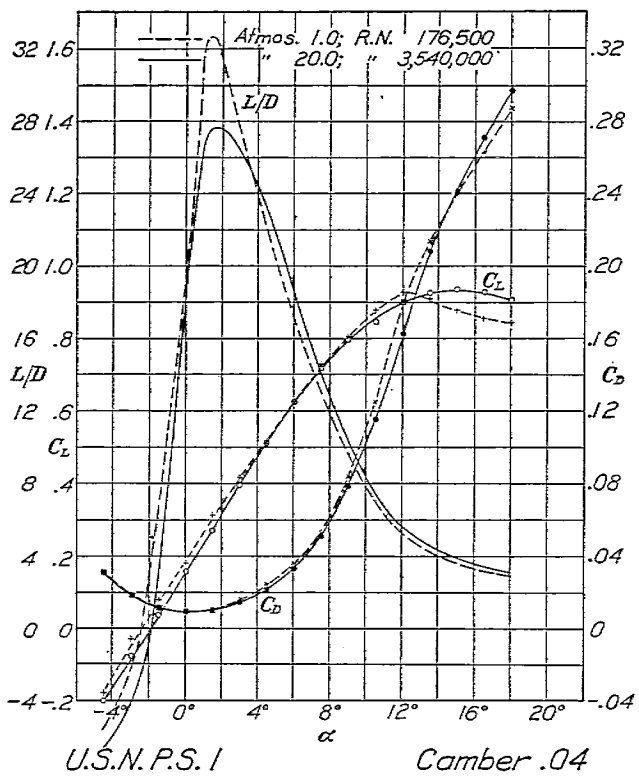


FIG. 13.—Characteristic curves of U. S. N. P. S. 1 at different values of R. N.

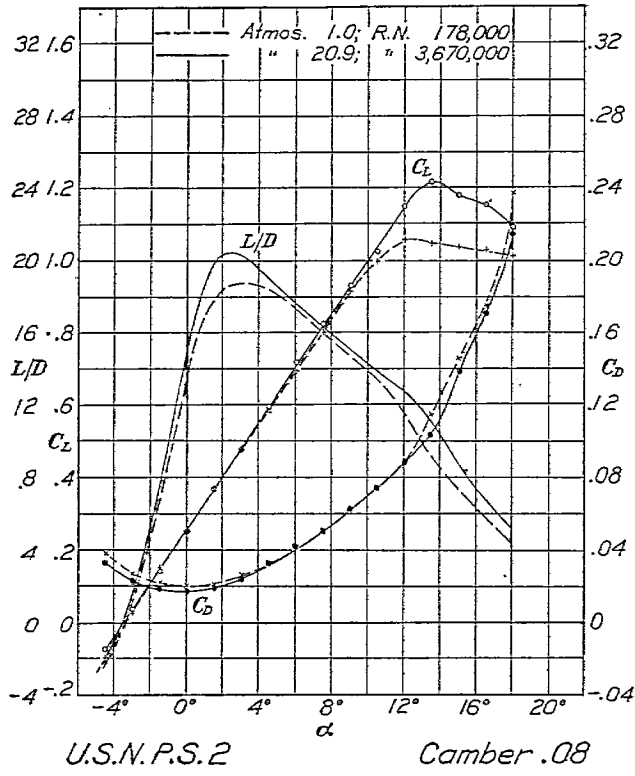


FIG. 14.—Characteristic curves of U. S. N. P. S. 2 at different values of R. N.

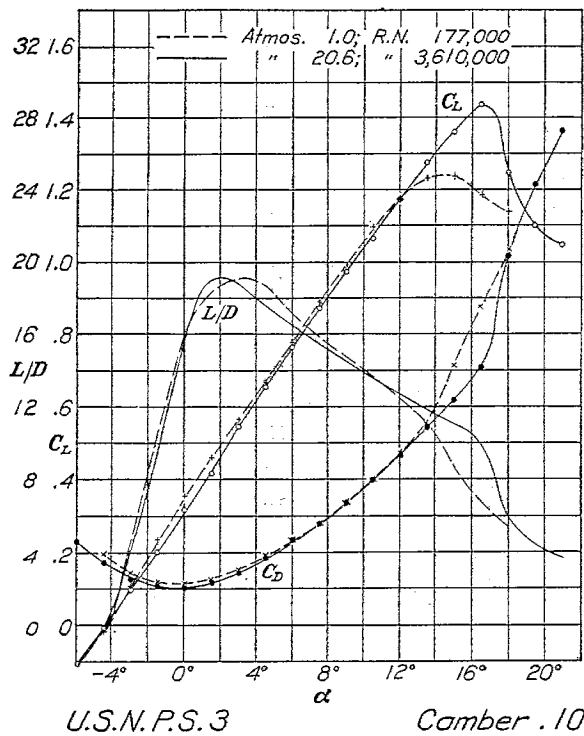


FIG. 15.—Characteristic curves of U. S. N. P. S. 3 at different values of R. N.

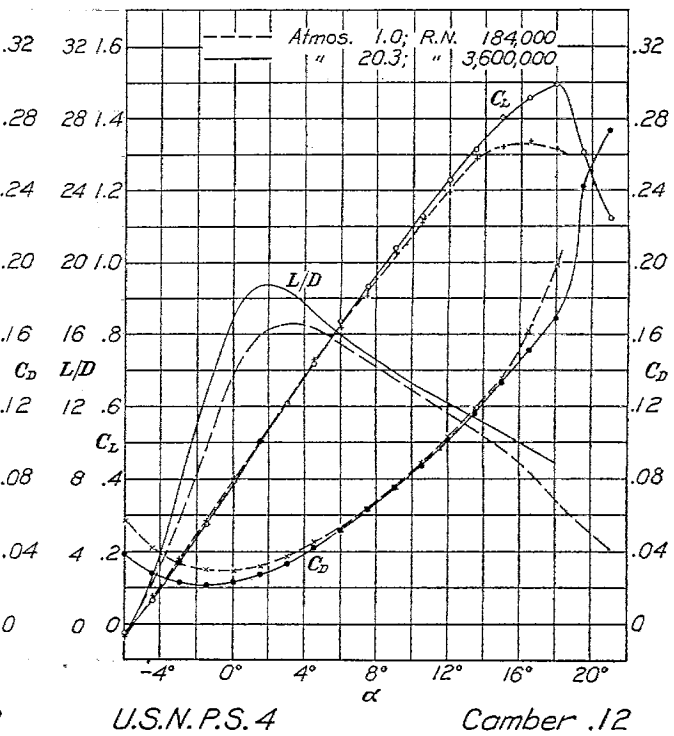


FIG. 16.—Characteristic curves of U. S. N. P. S. 4 at different values of R. N.

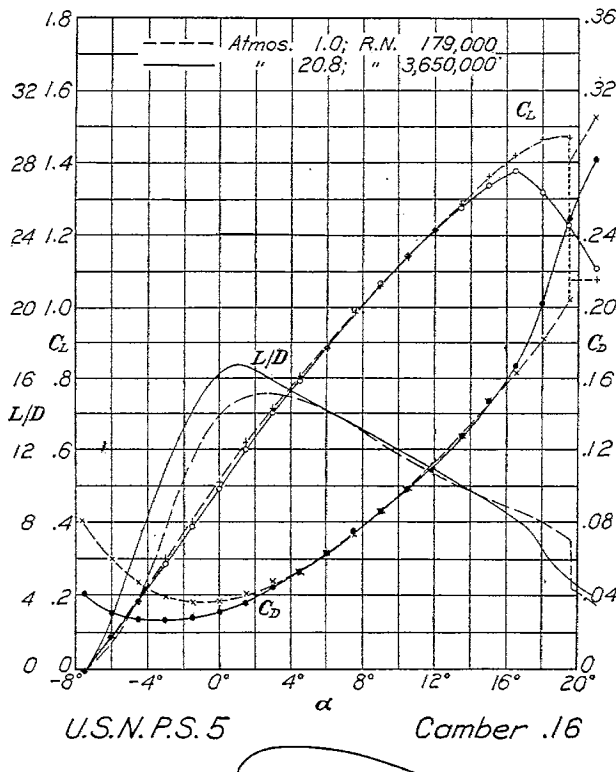


FIG. 17.—Characteristic curves of U. S. N. P. S. 5 at different values of R. N.

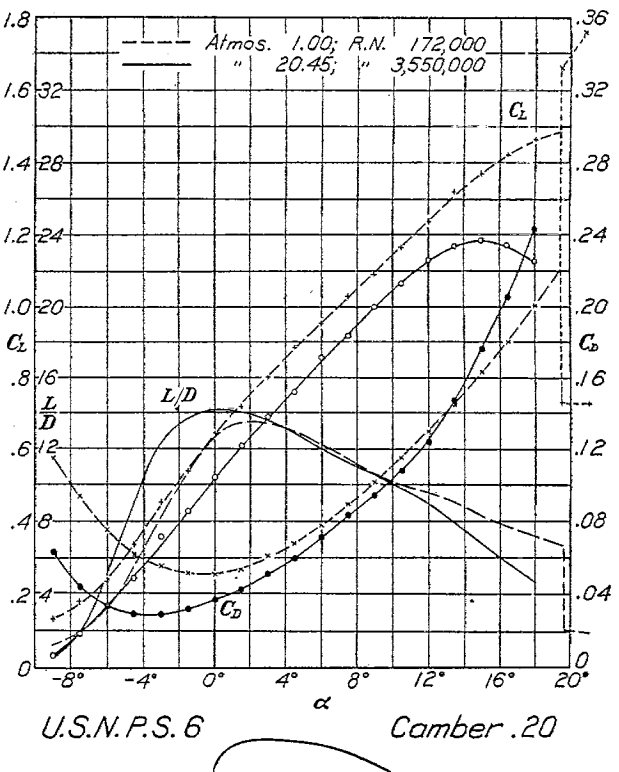


FIG. 18.—Characteristic curves of U. S. N. P. S. 6 at different values of R. N.

Reference 2. The results of these calculations, together with the data as found from the experiments, for comparison, are given in Table II. The agreement is certainly very striking if allowance is made for the errors of measurement and for the assumptions and approximations made in the derivation of the theory. It would appear from Table II that the moment coefficient and the angle of zero lift may be calculated from the ordinates of a section to an accuracy sufficient for most engineering work. The slope of the lift curve, however, departs noticeably from the computed values and in such a way as to be consistent with all other measurements made in this tunnel. This subject will be taken up in a technical note.

## REFERENCES

- No. 1. Munk, Max M., and Miller, Elton W.: The Variable Density Wind Tunnel of the National Advisory Committee for Aeronautics. N. A. C. A. Technical Report No. 227, 1926.
- No. 2. Munk, Max M.: The Determination of the Angles of Attack of Zero Lift and of Zero Moment, Based on Munk's Integrals. N. A. C. A. Technical Note No. 122, 1923.
- No. 3. Caldwell, F. W., and Fales, E. N.: Wind Tunnel Studies in Aerodynamic Phenomena at High Speed. N. A. C. A. Technical Report No. 83, 1920.
- No. 4. Briggs, L. J., and Dryden, H. L., Aerodynamic Characteristics of Airfoils at High Speed. N. A. C. A. Technical Report No. 207, 1925.

TABLE I  
SPECIFIED ORDINATES OF UPPER SURFACE OF PROPELLER SECTIONS IN FRACTIONS OF CHORD

Lower Surfaces are Flat

Section-----	1	2	3	4	5	6
Camber-----	0.04	0.08	0.10	0.12	0.16	0.20
L. Edge Rad-----	0.0040	0.0080	0.0100	0.0120	0.0160	0.0200
0.025 Sta-----	.0164	.0328	.0410	.0492	.0656	.0820
.05 Sta-----	.0236	.0472	.0590	.0708	.0944	.1180
.075 Sta-----	.0283	.0566	.0708	.0850	.1133	.1416
.10 Sta-----	.0316	.0632	.0790	.0948	.1265	.1580
.15 Sta-----	.0358	.0716	.0895	.1074	.1482	.1790
.20 Sta-----	.0380	.0760	.0950	.1140	.1520	.1900
.30 Sta-----	.0399	.0798	.0998	.1198	.1597	.1996
.40 Sta-----	.0396	.0792	.0990	.1188	.1584	.1980
.50 Sta-----	.0380	.0760	.0950	.1140	.1520	.1900
.60 Sta-----	.0348	.0696	.0870	.1044	.1392	.1740
.70 Sta-----	.0296	.0592	.0740	.0888	.1184	.1480
.80 Sta-----	.0224	.0448	.0560	.0672	.0896	.1120
.90 Sta-----	.0142	.0282	.0352	.0423	.0563	.0704
.95 Sta-----	.0098	.0197	.0246	.0295	.0394	.0492
T. Edge Rad-----	.0031	.0062	.0092	.0077	.0123	.0154

TABLE II  
COMPUTED ANGLE OF ZERO LIFT AND MOMENT COEFFICIENT

Section No.	Maximum thickness	Angle of zero lift		Moment coefficient	
		Predicted	Found from experiment	Predicted	Average value from experiment
1	0.04	Degrees -1.6	Degrees -2.0	-0.024	-0.012
2	.08	-3.3	-3.4	-.052	-.065
3	.10	-4.1	-4.3	-.064	-.075
4	.12	-5.2	-5.5	-.080	-.088
5	.16	-7.0	-7.4	-.108	-.110
6	.20	-8.6	-10.0	-.131	-.145

TABLE III  
Section No. U. S. N. P. S. 1. Test No. 176-7.  
Average pressure, 1 atmos. Chord, 5 in. (12.7 cm).  
Average dynamic pressure, 28 kg/m<sup>2</sup>. Span, 30 in. (76.2 cm).  
Average temperature, 24° C. Aspect ratio, 6.  
Average Reynolds Number 176,500. Area, 0.0968 m<sup>2</sup>.

Angle of attack degrees	Lift coefficient $C_L$	Drag coefficient $C_D$	Ratio $\frac{L}{D}$	Moment coefficient $C_M$
-4.5	-0.180	0.0319	-5.64	+0.021
-3.0	-.030	.0178	-1.68	-.029
-1.5	+.078	.0114	6.84	-.009
0	.181	.0096	18.85	-.055
+1.5	.313	.0096	32.60	-.029
3	.417	.0152	27.43	-.049
4.5	.515	.0249	20.68	-.045
6	.626	.0354	17.68	-.038
7.5	.729	.0517	14.10	-.024
9	.806	.0837	9.63	-.063
10.5	.877	.1244	7.05	-.087
12	.929	.1798	5.17	-.069
13.5	.907	.2136	4.25	-.086
15	.877	.2404	3.65	-.089
16.5	.855	.2631	3.25	-.098
18	.844	.2873	2.94	-.085

TABLE IV

Section No. U. S. N. P. S. 1.  
 Average pressure, 20.0 atmos.  
 Average dynamic pressure, 618 kg/m<sup>2</sup>.  
 Average temperature, 35° C.  
 Average Reynolds Number 3,540,000.

Test No. 146-4.  
 Chord, 5 in. (12.7 cm).  
 Span, 30 in. (76.2 cm).  
 Aspect ratio, 6.  
 Area, 0.0968 m<sup>2</sup>.

Angle of attack degrees	Lift coefficient $C_L$	Drag coefficient $C_D$	Ratio $\frac{L}{D}$	Moment coefficient $C_M$
-4.5	-0.202	0.0300	-6.73	-0.004
-3	-0.078	.0179	-4.36	-.017
-1.5	+.035	.0112	3.12	-.013
0	.155	.0086	18.02	-.014
+1.5	.270	.0098	27.55	+.020
3	.397	.0152	26.12	+.007
4.5	.512	.0216	23.70	-.005
6	.623	.0328	18.99	-.007
7.5	.713	.0507	14.06	+.002
9	.797	.0787	10.13	+.004
10.5	.845	.1154	7.32	+.005
12	.898	.1624	5.53	-.038
13.5	.924	.2035	4.54	-.072
15	.933	.2410	3.87	-.100
16.5	.930	.2715	3.42	-.111
18	.908	.2971	3.06	-.111

TABLE V

Section No. U. S. N. P. S. 2.  
 Average pressure, 1 atmos.  
 Average dynamic pressure, 28.5 kg/m<sup>2</sup>.  
 Average temperature, 24° C.  
 Average Reynolds Number 178,000.

Test No. 151-2.  
 Chord, 5 in. (12.7 cm).  
 Span, 30 in. (76.2 cm).  
 Aspect ratio, 6.  
 Area, 0.0968 m<sup>2</sup>.

Angle of attack degrees	Lift coefficient $C_L$	Drag coefficient $C_D$	Moment coefficient $C_M$	Ratio $\frac{L}{D}$
-4.5	-0.101	0.0388	-0.084	-2.60
-3	+.051	.0268	-.040	1.90
-1.5	.149	.0223	-.067	6.68
0	.258	.0202	-.096	12.77
+1.5	.374	.0210	-.051	17.81
3	.477	.0258	-.075	18.49
4.5	.578	.0314	-.053	18.41
6	.694	.0402	-.027	17.26
7.5	.799	.0504	-.061	15.85
9	.912	.0615	-.055	14.83
10.5	.995	.0740	-.033	13.45
12	1.054	.0880	-.013	11.98
13.5	1.043	.1140	+.029	9.15
15	1.032	.1443	+.015	7.15
16.5	1.028	.1748	+.003	5.88
18	1.010	.2369	-.024	4.26

TABLE VI

Section No. U. S. N. P. S. 2. Test No. 151-3.  
 Average pressure, 20.9 atmos. Chord, 5 in. (12.7 cm).  
 Average dynamic pressure, 650 kg/m<sup>2</sup>. Span, 30 in. (6.2 cm).  
 Average temperature, 38° C. Aspect ratio, 6.  
 Average Reynolds Number, 3,670,000. Area, 0.0968 m<sup>2</sup>.

Angle of attack degrees	Lift coefficient $C_L$	Drag coefficient $C_D$	Moment coefficient $C_M$	Ratio $\frac{L}{D}$
-4.5	-0.075	0.0331	-0.064	-2.27
-3	+.033	.0230	-.061	1.43
-1.5	.140	.0185	-.068	7.57
0	.252	.0173	-.072	14.57
+1.5	.367	.0185	-.068	19.84
3	.481	.0238	-.056	20.21
4.5	.594	.0324	-.088	18.33
6	.717	.0415	-.076	17.28
7.5	.822	.0496	-.064	16.57
9	.927	.0622	-.034	14.90
10.5	1.021	.0737	-.107	13.85
12	1.143	.0880	-.054	12.99
13.5	1.215	.1033	-.072	11.76
15	1.178	.1411	-.101	8.35
16.5	1.151	.1701	-.093	6.77
18	1.090	.2141	-.118	5.09

TABLE VII

Section No. U. S. N. P. S. 3. Test No. 152-1.  
 Average pressure, 1 atmos. Chord, 5 in. (12.7 cm).  
 Average dynamic pressure, 28.4 kg/m<sup>2</sup>. Span, 30 in. (76.2 cm).  
 Average temperature, 27° C. Aspect ratio, 6.  
 Average Reynolds Number 177,000. Area, 0.0968 m<sup>2</sup>.

Angle of attack degrees	Lift coefficient $C_L$	Drag coefficient $C_D$	Ratio $\frac{L}{D}$	Moment coefficient $C_M$
-4.5	0.018	0.0399	0.45	-0.058
-3	.125	.0287	.4.35	-.096
-1.5	.236	.0228	10.35	-.099
0	.353	.0225	15.69	-.109
+1.5	.459	.0252	18.21	-.111
3	.564	.0301	18.74	-.143
4.5	.666	.0349	19.08	-.119
6	.779	.0449	17.35	-.116
7.5	.889	.0561	15.85	-.108
9	.990	.0669	14.80	-.087
10.5	1.095	.0801	13.67	-.054
12	1.179	.0950	12.41	-.069
13.5	1.230	.1101	11.17	-.047
15	1.237	.1420	8.71	-.038
16.5	1.183	.1751	6.76	-.038
18	1.139	.2069	5.50	-.036

TABLE VIII

Section No. U. S. N. P. S. 3.  
 Average pressure, 20.6 atmos.  
 Average dynamic pressure, 640 kg/m<sup>2</sup>.  
 Average temperature, 38° C.  
 Average Reynolds Number 3,610,000.

Test No. 152-2.  
 Chord, 5 in. (12.7 cm).  
 Span, 30 in. (76.2 cm).  
 Aspect ratio, 6.  
 Area, 0.0968 m<sup>2</sup>.

Angle of attack degrees	Lift coefficient $C_L$	Drag coefficient $C_D$	Ratio $\frac{L}{D}$	Moment coefficient $C_M$
-6	-0.106	0.0461	-2.30	0.066
-4.5	-0.011	.0341	-0.32	-.073
-3	+.098	.0253	3.87	-.072
-1.5	.202	.0217	9.31	-.068
0	.317	.0204	15.54	-.067
+1.5	.431	.0227	18.99	-.073
3	.543	.0288	18.85	-.082
4.5	.652	.0374	17.43	-.095
6	.762	.0467	16.32	-.097
7.5	.870	.0557	15.62	-.070
9	.972	.0663	14.66	-.085
10.5	1.065	.0792	13.45	-.090
12	1.174	.0923	12.72	-.066
13.5	1.277	.1079	11.83	-.077
15	1.359	.1231	11.04	-.089
16.5	1.438	.1416	10.15	-.083
18	1.247	.2034	6.18	-.081
19.5	1.100	.2430	4.53	-.114
21	1.047	.2730	3.83	-.106

TABLE IX

Section No. U. S. N. P. S. 4.  
 Average pressure, 1 atmos.  
 Average dynamic pressure, 29.34 kg/m<sup>2</sup>.  
 Average temperature, 22° C.  
 Average Reynolds Number 184,000.

Test No. 153-1.  
 Chord, 5 in. (12.7 cm).  
 Span, 30 in. (76.2 cm).  
 Aspect ratio, 6.  
 Area, 0.0968 m<sup>2</sup>.

Angle of attack degrees	Lift coefficient $C_L$	Drag coefficient $C_D$	Ratio $\frac{L}{D}$	Moment coefficient $C_M$
-6	-0.035	0.0576	-0.610	-0.015
-4.5	+.081	.0422	1.92	-.101
-3	.182	.0332	5.48	-.137
-1.5	.288	.0301	9.57	-.138
0	.400	.0292	13.70	-.121
+1.5	.509	.0320	15.90	-.113
3	.607	.0375	16.19	-.137
4.5	.710	.0432	16.43	-.093
6	.816	.0531	15.37	-.136
7.5	.908	.0631	14.39	-.134
9	1.028	.0759	13.54	-.092
10.5	1.110	.0888	12.50	-.079
12	1.198	.1033	11.60	-.076
13.5	1.296	.1218	10.64	-.043
15	1.322	.1357	9.74	-.025
16.5	1.336	.1612	8.29	+.007
18	1.315	.1991	6.60	+.035

TABLE X

Section No. U. S. N. P. S. 4.  
 Average pressure, 20.3 atmos.  
 Average dynamic pressure, 635 kg/m<sup>2</sup>.  
 Average temperature, 36° C.  
 Average Reynolds Number 3,600,000.

Test No. 153-2.  
 Chord, 5 in. (12.7 cm).  
 Span, 30 in. (76.2 cm).  
 Aspect ratio, 6.  
 Area, 0.0968 m<sup>2</sup>.

Angle of attack degrees	Lift coefficient $C_L$	Drag coefficient $C_D$	Ratio $\frac{L}{D}$	Moment coefficient $C_M$
-6	-0.028	0.0383	0.73	-0.086
-4.5	+.067	.0280	2.39	-.088
-3	.173	.0228	7.59	-.086
-1.5	.276	.0218	12.66	-.088
0	.393	.0235	16.72	-.089
+1.5	.506	.0272	18.60	-.088
3	.607	.0330	18.39	-.093
4.5	.718	.0420	17.09	-.095
6	.833	.0522	15.90	-.087
7.5	.932	.0633	14.72	-.088
9	1.041	.0748	13.92	-.088
10.5	1.127	.0865	13.03	-.094
12	1.230	.1017	12.09	-.083
13.5	1.314	.1158	11.35	-.087
15	1.403	.1331	10.54	-.088
16.5	1.456	.1506	9.67	-.090
18	1.492	.1689	8.83	-.100
19.5	1.308	.2424	5.40	-.097
21	1.121	.2734	4.10	-.106

TABLE XI

Section No. U. S. N. P. S. 5.  
 Average pressure, 1 atmos.  
 Average dynamic pressure, 28.8 kg/m<sup>2</sup>.  
 Average temperature, 25° C.  
 Average Reynolds Number 179,000.

Test No. 154-1.  
 Chord, 5 in. (12.7 cm).  
 Span, 30 in. (76.2 cm).  
 Aspect ratio, 6.  
 Area, 0.0968 m<sup>2</sup>.

Angle of attack degrees	Lift coefficient $C_L$	Drag coefficient $C_D$	Ratio $\frac{L}{D}$	Moment coefficient $C_M$
-7.5	-0.007	0.0803	-0.09	-0.059
-6	+.082	.0599	1.37	-.073
-4.5	.189	.0473	4.00	-.130
-3	.299	.0389	7.70	-.150
-1.5	.401	.0358	11.20	-.167
0	.508	.0365	13.92	-.167
+1.5	.620	.0409	15.16	-.123
3	.709	.0478	14.83	-.114
4.5	.805	.0532	15.13	-.090
6	.885	.0633	13.98	-.115
7.5	.988	.0727	13.59	-.085
9	1.056	.0859	12.29	-.086
10.5	1.142	.0985	11.59	-.067
12	1.215	.1131	10.74	-.062
13.5	1.282	.1286	9.97	-.016
15	1.361	.1460	9.32	-.001
16.5	1.415	.1621	8.73	+.046
18	1.461	.1809	8.08	+.073
19.5	1.468	.2041	7.19	+.084
21	1.074	.3048	3.52	+.123

TABLE XII

Section No. U. S. N. P. S. 5.  
 Average pressure, 20.8 atmos.  
 Average dynamic pressure, 643 kg/m<sup>2</sup>.  
 Average temperature, 45° C.  
 Average Reynolds Number 3,650,000.

Test No. 154-2.  
 Chord, 5 in. (12.7 cm).  
 Span, 30 in. (76.2 cm).  
 Aspect ratio, 6.  
 Area, 0.0968 m<sup>2</sup>.

Angle of attack degrees	Lift coefficient $C_L$	Drag coefficient $C_D$	Ratio $\frac{L}{D}$	Moment coefficient $C_M$
-7.5	-0.005	0.0406	-0.01	-0.113
-6	.086	.0295	2.91	-.113
-4.5	.182	.0267	6.82	-.112
-3	.287	.0266	10.79	-.111
-1.5	.389	.0277	14.04	-.110
0	.492	.0303	16.24	-.116
+1.5	.599	.0357	16.78	-.113
3	.701	.0442	15.86	-.117
4.5	.792	.0526	15.06	-.106
6	.883	.0614	14.38	-.112
7.5	.992	.0744	13.33	-.106
9	1.065	.0849	12.54	-.088
10.5	1.143	.0973	11.75	-.082
12	1.212	.1114	10.88	-.093
13.5	1.274	.1271	10.02	-.100
15	1.338	.1469	9.11	-.095
16.5	1.376	.1663	8.27	-.102
18	1.319	.2019	6.53	-.079
19.5	1.228	.2482	4.95	-.107
21	1.103	.2810	3.92	-.090

TABLE XIII

Section No. U. S. N. P. S. 6.  
 Average pressure, 1 atmos.  
 Average dynamic pressure, 27.3 kg/m<sup>2</sup>.  
 Average temperature, 27° C.  
 Average Reynolds Number 172,000.

Test No. 155-2.  
 Chord, 5 in. (12.7 cm).  
 Span, 30 in. (12.7 cm).  
 Aspect ratio, 6.  
 Area, 0.0968 m<sup>2</sup>.

Angle of attack degrees	Lift coefficient $C_L$	Drag coefficient $C_D$	Ratio $\frac{L}{D}$	Moment coefficient $C_M$
-18	0.034	0.2042	0.17	+0.015
-15	.117	.1656	.71	-.148
-12	.159	.1383	1.15	-.168
-9	.159	.1141	1.39	-.110
-7.5	.178	.0936	1.90	-.162
-6	.232	.0742	3.13	-.216
-4.5	.337	.0607	5.55	-.203
-3	.452	.0547	8.26	-.187
-1.5	.538	.0509	10.57	-.181
0	.642	.0503	12.76	-.145
+1.5	.717	.0529	13.55	-.144
3	.800	.0606	13.20	-.128
4.5	.883	.0675	13.08	-.078
6	.951	.0770	12.35	-.114
7.5	1.029	.0890	11.56	-.121
9	1.089	.1012	10.76	-.120
10.5	1.164	.1146	10.16	-.132
12	1.238	.1286	9.63	-.110
13.5	1.315	.1443	9.11	-.155
15	1.357	.1629	8.33	-.184
16.5	1.420	.1799	7.89	-.179
18	1.462	.2004	7.29	-.170
19.5	.728	.3323	2.19	-.129
21	.727	.3585	2.03	-.082

TABLE XIV

Section No. U. S. N. P. S. 6.  
 Average pressure, 20.45 atmos.  
 Average dynamic pressure, 628 kg/m<sup>2</sup>.  
 Average temperature, 39° C.  
 Average Reynolds Number 3,550,000.

Test No. 155-3.  
 Chord, 5 in. (12.7 cm).  
 Span, 30 in. (76.2 cm).  
 Aspect ratio, 6.  
 Area, 0.0968 m<sup>2</sup>.

Angle of attack degrees	Lift coefficient $C_L$	Drag coefficient $C_D$	Ratio $\frac{L}{D}$	Moment coefficient $C_M$
-10.5	-0.006	0.0880	-0.01	-0.119
-9	+.028	.0624	0.45	-.077
-7.5	.088	.0433	2.03	-.134
-6	.164	.0325	5.05	-.128
-4.5	.241	.0284	8.49	-.131
-3	.356	.0281	12.67	-.075
-1.5	.426	.0314	13.57	-.114
0	.517	.0363	14.24	-.115
+1.5	.604	.0426	14.18	-.108
3	.688	.0502	13.70	-.102
4.5	.758	.0587	12.91	-.100
6	.853	.0705	12.10	-.099
7.5	.916	.0824	11.12	-.129
9	.999	.0939	10.64	-.083
10.5	1.062	.1067	9.95	-.092
12	1.129	.1232	9.16	-.091
13.5	1.168	.1464	7.98	-.095
15	1.181	.1755	6.73	-.113
16.5	1.170	.2053	5.70	-.112
18	1.124	.2482	4.62	-.094